

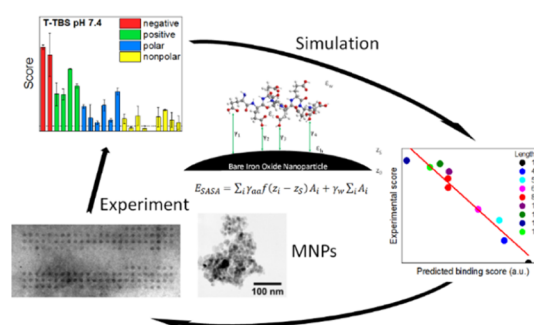
Rational Design of Iron Oxide Binding Peptide Tags

Sebastian Patrick Schwaminger,[†] Priya Anand,[‡] Monika Borkowska-Panek,[‡] Silvia Angela Blank-Shim,[†] Paula Fraga-García,[†] Karin Fink,[‡] Sonja Berensmeier,^{*,†} and Wolfgang Wenzel^{*,‡}

[†]Bioseparation Engineering Group, Department of Mechanical Engineering, Technical University of Munich, Boltzmannstraße 15, 85748 Garching, Germany

[‡]Institute of Nanotechnology, Karlsruhe Institute of Technology, 76344 Eggenstein Leopoldshafen, Germany

ABSTRACT: Owing to their extraordinary magnetic properties and low cost production, iron oxide nanoparticles (IONs) are in the focus of research. In order to better understand interactions of IONs with biomolecules, a tool for the prediction of the propensity of different peptides to interact with IONs is of great value. We present an effective implicit surface model (EISM), which includes several interaction models. Electrostatic interactions, van der Waals interactions, and entropic effects are considered for the theoretical calculations. However, the most important parameter, a surface accessible area force field contribution term, derives directly from experimental results on the interactions of IONs and peptides. Data from binding experiments of ION agglomerates to different peptides immobilized on cellulose membranes have been used to parameterize the model. The work was carried out under defined environmental conditions; hence, effects because of changes, for example structure or solubility by changing the surroundings, are not included. EISM enables researchers to predict the binding of peptides to IONs, which we then verify with further peptide array experiments in an iterative optimization process also presented here. Negatively charged peptides were identified as best binders for IONs in Tris buffer. Furthermore, we investigated the constitution of peptides and how the amount and position of several amino acid side chains affect peptide binding. The incorporation of glycine leads to higher binding scores compared to the incorporation of cysteine in negatively charged peptides.



INTRODUCTION

Biomolecular recognition plays an important role in nature as well as in modern industrial applications.^{1–3} Receptors, which are present in the human body from nose to liver and vary depending on their function, recognize different biomolecules or biomolecule sequences.⁴ The interaction between inorganic and organic tissue in biological systems is often mediated by proteins and peptides.^{2,5,6} Therefore, the development of new methods of biomolecular recognition and the design of short affinity binding amino acid sequences, so called tags, are of great importance for purification, detection, immobilization, or separation in protein science.^{7,8} Moreover, the applications of such affinity tag based systems extend to other fields, from downstream processing to medical in vivo applications such as drug delivery.^{9,10} An affinity tag usually has a specific counterpart to which it can bind.¹¹ Here, superparamagnetic iron oxide nanoparticles (IONs) come into play. IONs are easy to synthesize at low costs. Their superparamagnetic behavior allows for their manipulation by an external magnetic field to easily accumulate IONs in a desired area.^{12,13} Drug delivery,¹⁰ hyperthermia treatment,¹⁴ and magnetic resonance imaging^{15,16} are among the multiple biomedical applications, which can be based on magnetic nanoparticles. Even in

complex biological environments, affinity tags help modify and stabilize particles with different drugs or other biomolecules as the target goal.¹¹ In biotechnology, IONs are used as a carrier material for enzymes,^{17–19} for DNA/RNA and protein purification,^{9,20–23} and for cell labeling and separation.²⁴ Selective tags lead to increased process efficiency while reducing costs and are therefore of great interest.²⁵

A rational design of peptide–surface interactions would normally start with a full quantitative characterization of surface interactions with amino acids, as peptide building blocks, and then proceed to treat collective effects. Unfortunately, no such quantitative model exists for IONs.²⁶ The greatest challenge for experimental approaches is the number of possible amino acid combinations, which is astronomical even for short sequences (≤ 20 amino acids).¹² Additionally, the interaction of amino acids at the solid/liquid interface of nanoscale surfaces is not yet wholly understood and difficult to analyze because of analytical limitations and the

complexity of these systems, which cannot be easily described using simple electrostatic models.^{3,12,26–28}

However, a number of possibilities exist to investigate the binding of peptide sequences to iron oxide surfaces and rationally develop new ION binding tags. The key to the design of high affinity peptide tags lies in an in depth understanding of surface–peptide recognition patterns.^{12,29} Our approach is to combine modeling with experimental data. Simulations of larger peptides (>20 amino acids) binding to complex surfaces are struggling presently both with the description of the surface in terms of a classical force field and the time scales involved in the rearrangement of the peptide when it binds to the surface.^{30,31} The first problem is particularly pertinent because for the relevant iron oxide surfaces available there is not even an atomistic model, which could be used to parameterize a classical interaction model. In prior work, we demonstrated that for some surfaces (gold, silver, silica, and TiO₂) it is possible to parameterize an implicit solvent implicit surface model that builds on an established all atom model for the peptide.³² The model is based on force fields representing the interaction between peptides and the nanoparticle surface and has enabled us to describe peptide binding to inorganic surfaces, such as gold. Here, because of the lack of an atomistic model for the surface, we are undertaking a different approach, the effective implicit surface model (EISM), which is parameterized by data from peptide arrays incubated with IONs.³² EISM is an example of an implicit model of the surface with a computational protocol based on the SIMONA engine,^{33,34} performing Monte Carlo calculations supported by metadynamics, employing force field methods as a system description. EISM has been parameterized for several surfaces using empirical data as a basis for defining the affinity of amino acids to inorganic surfaces in certain experimental conditions.³² For the binding, several types of interactions such as electrostatic interactions, hydrogen bonds, van der Waals interactions, and conformation effects are considered.

Hence, apart from the peptide sequence, many different factors, such as solvent composition, temperature, pH, and the presence of buffer molecules, have to be included.^{35–37} Emami et al. followed a similar approach to ours, varying the pH to predict the peptide binding to silica nanoparticles by the use of force fields.^{38,39} Peptide arrays can be utilized to develop new affinity tags for metals and metal oxides and are, therefore, useful for the parameterization of computational models.^{12,40–42} This technique is particularly well suited for the current study, as ION agglomerates stain distinctively, leaving dark spots, when bound to peptides on a white cellulose membrane.¹² Our group has recently achieved a first screening of 20 natural amino acid homo hexamer peptides with peptide arrays and found that the buffer and charged side chains exerted a strong influence on the peptide binding to magnetic IONs.¹²

The goal of this investigation is to extrapolate specific peptide–surface interactions from experimental results to rationally design ION binding peptide tags. We seek to provide a computer based platform of genetically engineered tags, which can be fused to proteins similar to established affinity tag systems (e.g. His tag, streptavidin tag, or FLAG tag) by identifying peptide sequences, specifically binding bare magnetite nanoparticles.

MATERIALS AND METHODS

Synthesis. All reagents were used as received from the manufacturer without further purification.

The bare IONs employed for this study were synthesized by co precipitation of Fe²⁺ and Fe³⁺ in alkaline aqueous solutions, consistent with our previously optimized procedure.⁴³ Therefore, 21.2 g of FeCl₃ × 6H₂O and 8.3 g of FeCl₂ × 4H₂O were dissolved in 200 mL of deionized, degassed water resulting in a Fe(III)/Fe(II) ratio of 1.9:1. This iron chloride solution was added to 1 L of 1 M NaOH prepared with deionized, degassed water stirred at 250 rpm in a reaction vessel. The reaction mixture was kept under a nitrogen atmosphere at 25 °C and stirred for an additional 30 min. The resulting nanoparticles were washed with deionized water until the conductivity of the solution was below 200 μS cm⁻¹. The solids were separated from the liquid using an NdFeB permanent magnet. The suspensions were lyophilized with an ALPHA 1 2 LD plus from Martin Christ Gefriertrocknungsanlagen GmbH, Germany, to obtain solid particles. FeCl₃ × 6H₂O and sodium hydroxide were purchased from AppliChem GmbH, Germany, at the highest purity available. FeCl₂·4H₂O extra pure was obtained from Merck KGaA, Germany.

Characterization. Transmission electron microscopy (TEM) images were recorded using a JEM 100 CX (JEOL GmbH, Germany). For the TEM measurements, the colloidal samples were diluted in degassed and deionized water, ultrasonicated to disperse any agglomerates and precipitated on carbon coated copper grids (Quantifoil Micro Tools GmbH, Germany). The pictures were manually processed in ImageJ. Thirty particles were measured in random order.

The crystal structure and phase purity of the lyophilized samples were examined with powder X ray diffraction (XRD). The measurements were performed with a STADI P diffractometer (STOE & Cie GmbH, Germany), equipped with a molybdenum source ($\lambda = 0.7093$ Å) and a Mythen IK detector (DECTRIS Ltd., Switzerland) in transmission geometry. Data were collected in the range from 2° to 50° (2 θ). The software package STOE WinXPOW (STOE & Cie GmbH, Germany) was used for indexing and refinement purposes.

Interaction Experiments. To determine the binding of peptides to bare IONs, CelluSpots peptide arrays from Intavis with 9.6 pmol of peptides per spot were used. The peptides were bound to the cellulose membrane via the C terminus; the free N terminus had previously been acetylated. The spot diameter was 2 mm. The membrane on which the peptides had been synthesized by the manufacturer was conditioned with 1 mL of methanol to rehydrate hydrophobic peptides.⁴⁴ Tris(hydroxymethyl)aminomethane (TBS) in double distilled water and supplemented with 137 mM NaCl and 2.7 mM KCl was used for the experiments. Tween 20 was added to a concentration of 0.25% (v/v) in the buffer to reduce nonspecific binding. The orbital shaker used for incubation was MultBio3D from Biosan.

The assay was conducted in the same way as described by Blank Shim et al.¹² Briefly, an array membrane was washed three times for 10 min each with 50 mL of buffer rotating of the orbital shaker at 30 rpm. After washing, the membrane was incubated for 60 min in a 0.4 g L⁻¹ ION suspension at the same rocking speed.⁴¹ The ION suspension was freshly prepared before the experiment by adding a buffer to lyophilized nanoparticles and sonicating for 15 min. Unbound particles were removed from the membrane by washing with the buffer three times for 10 min each. The membrane was then incubated in the buffer of interest for 1 h to test for reversible binding. The cellulose membrane was dried overnight at 4 °C; afterwards, an image was taken using a GelDoku station. To quantify the staining of the spots, the microarray profile plugin for ImageJ was used. The output of this plugin is a mean value of the spot darkness, which correlates to the amount of bound magnetic nanoparticles. An average value of the background was determined from 32 spots on the membrane without any peptides. The difference between this background value and the darkness of the peptide spots depends on the quantity of magnetic nanoparticles adsorbed by the peptides. Therefore, different shades of gray are an indicator of the binding

selectivity of the peptides pertaining to the IONs. The standard deviation was calculated for the darkness values of these 32 spots without any peptides to determine the background noise. For each experiment, this noise level is indicated as a dashed horizontal line in the respective figures. The membrane was regenerated in 100 mM oxalic acid for 40 min rotating on the orbital shaker after each use and washed for 10 min with double distilled water three times. Dried membranes were stored at $-20\text{ }^{\circ}\text{C}$ in a sealed plastic bag.

A buffered suspension of 0.4 g L^{-1} magnetic nanoparticles, as used in the peptide array binding assays described above, was sonicated for 15 min. The zeta potential was determined using the Smoluchowski equation in a Beckman Coulter Delsa Nano C at $25\text{ }^{\circ}\text{C}$. Each measurement was taken three times with 10 accumulations and a pinhole of $50\text{ }\mu\text{m}$.

Model. An effective implicit surface model (EISM) was used for fast and efficient *in silico* evaluation and prediction of peptide binding to the IONs. Previously, we had established an implicit solvent implicit surface model on the basis of an all atom model to describe peptide binding to inorganic surfaces such as gold.³² This model is based on force fields representing the interaction between peptides and the nanoparticle surface. The different forces responsible for the interactions are represented by the following terms

$$E = E_{\text{INT}} + E_{\text{SLIM}} + E_{\text{SLJ}} + E_{\text{SASA}} + E_{\text{PIT}}$$

The force field thus contains terms for the peptide internal energy (E_{INT}), electrostatic interactions (E_{SLIM}), Lennard Jones interactions (E_{SLJ}), solvent accessible surface area (E_{SASA}), and a pit potential (E_{PIT}), all of which are described in detail in the following.

The internal energy term is used to describe the internal interactions of peptides and not direct interaction with the surface. This term comprises standard force fields describing Lennard Jones, Coulomb, and dihedral interactions on the basis of the widely used AMBER99IDLN* force field.⁴⁵ This force field has been used in many studies to accurately describe the conformational ensemble of peptides, albeit in explicit solvent simulations.^{46,47} We have implemented an implicit solvent model based on the generalized Born model to further accelerate the simulations.^{45,48} We subdivided the system into several dielectric regions with various dielectric constants to not only describe the interactions of the peptide with the solvent, but also the interactions with the surface. For the nanoparticle surface the dielectric constant of magnetite ϵ_h ($\epsilon_h = 34.5$) is used, the peptide is assigned a dielectric constant ϵ_c ($\epsilon_c = 1$), and for the solvent the dielectric constant of water ϵ_w at ambient conditions is used ($\epsilon_w = 80$).

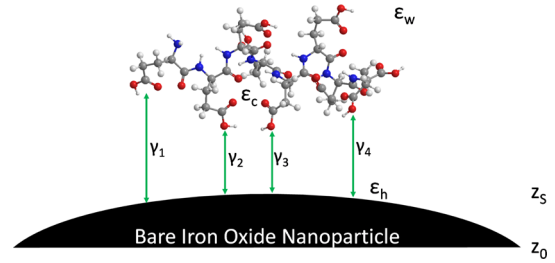
The van der Waals and Pauli exclusion interactions between the surface, which is assumed to be flat on the scale of the peptide, and the peptide are described by the Lennard Jones potential E_{SLJ} , which is shown in the equation below.

$$E_{\text{SLJ}} = 8 \sum_i \sqrt{\epsilon_i \cdot \epsilon_s} \cdot \left(\left(\frac{0.5 \cdot (\sigma_i + \sigma_s)}{z_i - z_s - \sigma_s} \right)^{12} - \left(\frac{0.5 \cdot (\sigma_i + \sigma_s)}{z_i - z_s - \sigma_s} \right)^6 \right)$$

The Lennard Jones potential is dependent on the distance between the surface and the peptide atoms z_s . Furthermore, the potential is composed of the Lennard Jones parameters of the surface ($\sigma_s = 3.5\text{ \AA}$ and $\epsilon_s = 0.1\text{ kcal mol}^{-1}$) and all peptide atoms (σ_i and ϵ_i). The terms described thus far model the peptide and a part of the interactions of the peptide and the surface, but neglect the presence of specific surface properties that depend on the specific surface and buffer under consideration. To incorporate these terms, we define an additional potential, E_{SASA} , which is proportional to the part of the solvent accessible surface of each amino acid that is in contact with the surface (Scheme 1). When the peptide is not in contact with the surface this potential is zero.

The interactions of individual amino acid contributions beyond the electrostatic and Lennard Jones terms are modeled by an amino acid specific interaction constant (γ) that must be determined particularly for each surface and interaction condition. The functional form of the SASA term for the model is then given as

Scheme 1. Illustration of Peptide Surface Interactions with the Parameters Implemented in the EISM



$$E_{\text{SASA}} = \sum_i \gamma_{\text{aa}} f(z_i - z_s) A_i + \gamma_w \sum_i A_i$$

The interaction of the amino acid with the surface is at full strength when the amino acid is close to the surface and gradually switched off at a given distance (z_s). The amino acid specific surface tension parameters (γ_{aa}),⁴⁹ which describe the interaction of all 20 individual amino acids with the surface, can either be obtained from explicit surface explicit solvent calculations of individual amino acids or correlated to experimental data. In the absence of an atomistic model for the surface we resorted to the latter approach here. To model the binding of the peptide to a surface, the peptides are confined in a finite box in all atom simulations to avoid allowing the peptide to diffuse away from the surface and to define an effective concentration. For this purpose, we use a pit potential (E_{PIT}) to restrict the position of the center of mass for the peptide chain to a given cubic box around the origin. If the center of mass is outside the binding box, a penalty function, increasing quadratically with the distance from the cubic box, is applied.

Calculation Protocols. All EISM simulations were performed using SIMONA,³³ a Monte Carlo based molecular simulation software implementing the EISM force field. SIMONA is freely available to academic users (<http://int.kit.edu/nanosim/simona>). The binding score for each peptide was computed using Monte Carlo simulation in the EISM model with 4 million simulation steps per simulation at 300 K using the metadynamics protocol implemented in PLUMED. For the metadynamics simulations, we used a single dimensional reaction coordinate adding Gaussians of width 0.1 and height 0.005 kJ mol^{-1} every 20th simulation step. We use the sum hills tool in PLUMED to calculate the free energy of binding.³⁴ The binding affinity of a particular peptide is characterized by the difference in Gibbs free energy between the bound and the unbound states. To reduce the numerical error, we averaged the predicted binding score over 20 independent simulations for every single peptide sequence.

RESULTS AND DISCUSSION

Experimental Data. The IONs used in this investigation have been characterized thoroughly in earlier works.^{12,50} Here, we want to emphasize the measurement of the surface potential which yielded a point of zero charge around pH 8 and therefore demonstrates the amphiphilic character of the ION surface.⁵¹ However, specific buffer effects, as described by Blank Shim et al., strongly affect the adsorption of peptides.¹² These effects are implemented in the EISM description for the ION surface. Other important nanoparticle properties affecting the adsorption and handling are their size, shape, and chemical composition, which define further physical properties, such as magnetization, specific surface area, and density.¹² The particles are mostly spherically shaped with a TEM diameter of around 13.5 nm and a Scherrer diameter of 8.3 nm . The nanoparticles are agglomerated in TBS buffer demonstrating a hydrodynamic diameter of around $2\text{ }\mu\text{m}$ (Figure S1). They consist mainly of magnetite, which can be verified with Raman

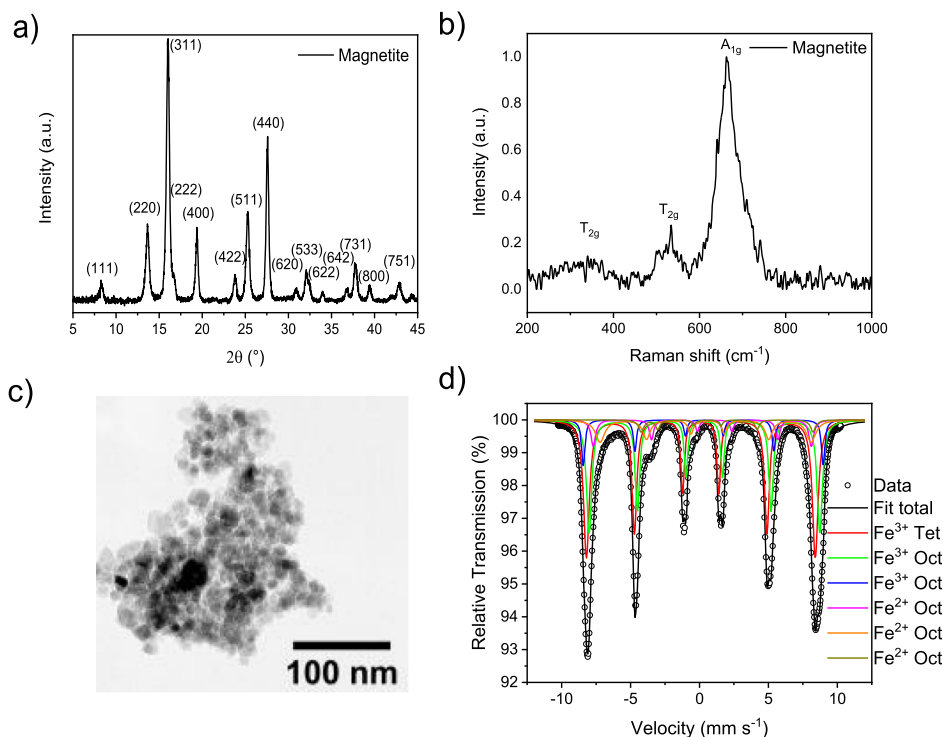


Figure 1. XRD of magnetite nanoparticles (a), Raman spectrum of magnetite nanoparticles at low laser powers (b), TEM image of nanoparticles (c), and Mössbauer spectrum of IONs (d) adapted from Blank Shim et al.¹²

spectroscopy, Mössbauer spectroscopy, as well as XRD (Figure 1).¹²

The nature, history, and environment of the particles define the interaction at the nano–bio interface. Under the chosen environmental conditions (50 mM Tris buffer at pH 7.4), the IONs are close to their isoelectric point and show a zeta potential of +3.7 mV.¹² Direct interactions between peptides and the surface, as well as interactions mediated by buffer ions (e.g., chloride), can occur. The interaction of IONs with carboxylic groups has been described for glutamic and aspartic acid based peptides at unbuffered conditions.^{25,52} On the other hand, interactions between positively charged peptides, such as lysine and arginine homomers and IONs, have been observed as well^{23,53} and these observations form the fundament for the EISM. The force fields are implemented with the scores determined by Blank Shim et al.¹² To implement the SASA term, the binding scores of magnetite nanoparticles to homo hexapeptides were investigated. Figure 2 shows the binding scores at pH 7.4 in Tris buffered saline. Here, especially the binding of negatively charged peptides can be observed. However, the other peptides, containing positive charges as well, even though the binding scores are lower. For polar and nonpolar peptides, the binding depends on the particular amino acid subunits. Peptides containing cysteine, histidine, serine, tyrosine, or proline bind magnetite at least to some extent.

Parameterization of the Model. As described in the methods section, the EISM model needs to be parameterized either by all atom simulations using an explicit surface representation or by experimental data. Here, we use the data in Figure 2, specifically the log of the binding score, as a measure of the binding of the homo peptides. The experimental binding score in Table 1 leads to the amino acid specific surface tension parameter γ_{aa} . To this end, we

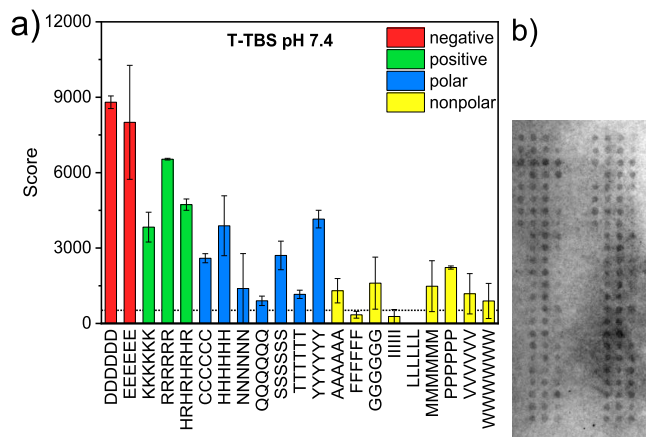


Figure 2. Photometric binding scores of magnetite nanoparticles (0.4 g L⁻¹) in Tris buffered saline (pH 7.4) bound to different homo hexapeptides (a). Photograph of peptide array (b). A table listing the array configuration can be found in the Supporting Information.

performed EISM simulations using different values of γ_{aa} for each homo peptide until the computed binding score matched the experimentally observed score. We use the term “surface tension” because the term is proportional to the change in the surface when the peptide comes into contact with the surface. In the EISM model the electrostatic interactions of the peptide with the surface are modeled by an implicit electrostatic (generalized Born) model, which treats the surface as a homogenous slab. Deviations from this model and all contact interactions that may arise through the contact of amino acids with specific groups on the surface are modeled by the surface tension term. Because the free energy of binding cannot be determined from the experiment, there is an unknown proportionality constant. For this reason, we cannot compare

Table 1. Binding Scores of Homo Hexapeptides for All 20 Amino Acids and the Resulting SASA Parameter γ_{aa} Which Was Used To Predict the Binding Scores at the Aqueous Interface of IONs

amino acid	experimental score (6 \times)	γ_{aa}	amino acid	experimental score (6 \times)	γ_{aa}
Ala	1301	0	Leu	0	0
Arg	6537	0.054	Lys	3833	0.047
Asn	1390	0.013	Met	1483	0.017
Asp	8801	0.075	Phe	345	0
Cys	2595	0	Pro	2226	0
Gln	901	0	Ser	2706	0.0228
Glu	8003	0.072	Thr	1159	0
Gly	1603	0.011	Trp	895	0
His	3887	0.041	Tyr	4154	0.0186
Ile	277	0	Val	1181	0

absolute free energy differences, but only scores obtained either from theory or experiment.

At a later stage, we will use the model to rank other peptides by the same experimental procedure. Prior to the parameterization of the model, a score value of 1500 was subtracted from all experimental scores, as this value is seen as corresponding to unspecific binding of the peptide to the membrane. This background noise can be observed as mean darkness by particle staining on the membrane, where no peptides are spotted (Figure 2b). Table 1 lists the experimental data for the homo hexamers on magnetite nanoparticles, and the resulting surface tension parameters for each amino acid following this procedure. In light of the surface tension parameter of the EISM model these data indicate that there are some amino acids, for example alanine, proline, and serine, for which the interactions of the peptide with the surface are sufficiently described with the continuum electrostatic model of the surface. For other amino acids, such as glutamic acid, arginine and aspartic acid, the fit to the experimental data can only be accomplished when additional interactions are included in the model. These most likely arise from charges/charge sites on the surface which provide enhanced binding of these amino acids to the surface. For some amino acids, such as serine and tyrosine, these contact interactions are repulsive.

Validation of the Model for Complex Peptides. We have parameterized an implicit solvent, implicit surface model for the interactions of peptides with the iron oxide surface. In principle, this model can now be used to compute the adsorption of arbitrary peptides to the same surface under the same environmental conditions. The remainder of this investigation is dedicated to answering the question of whether this transferability of the parameters, obtained for homo peptides, can indeed be achieved. If successful, the EISM model can be used as a ranking tool for characterizing the binding of arbitrary peptides to magnetite nanoparticles. We must stress, however, that the model is only applied to peptides binding to magnetite nanoparticles at the investigated buffer conditions. Whenever the buffer conditions are changed, the model at present must be reparameterized with new experimental data.

We have therefore performed experiments using different peptide sequences to validate the predicted adsorption free energies. This part of the investigation focuses on the effect of negatively charged amino acid subunits of peptides. In particular, the synergies with other amino acids, the amount

of negatively charged amino acids, as well as their position are investigated. The simulated binding scores of glutamate homo peptides to IONs are shown in Figure 3. As expected the

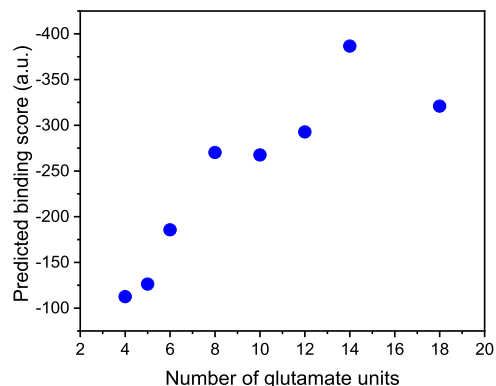


Figure 3. Comparison of the predicted binding scores for homo glutamic acid peptide sequences of different lengths.

predicted binding score tends to increase with an increasing number of glutamate subunits. However, there is no linear dependence and some smaller peptides even demonstrate a lower binding score than larger peptides.

A general trend toward higher binding scores with increasing numbers of glutamate or aspartate subunits can be confirmed when comparing the model results with experimental results from the peptide array experiments (Figure 4). We find that

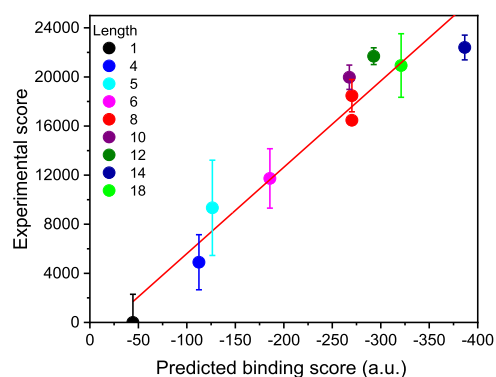


Figure 4. Comparison of the theoretically and the experimentally obtained binding scores for homo glutamic acid peptide sequences with different lengths.

the peptide containing 14 subunits of glutamate demonstrates a higher binding score than the peptide containing 18 subunits, as predicted by the model. Overall, we find a strong positive correlation ($R^2 = 0.94$) between the predicted and the experimental binding scores, which is a first indication of the transferability of the EISM model to more complex peptides.

Whereas the longer homo peptides tend to bind better, both in the model and the experiment, there are interesting deviations from a purely linear trend, which may stem from changes in conformation and synergies with other amino acid subunits.³¹

Thus, we investigated the behavior of peptides with similar chain lengths but different amino acid sequences, focusing on the influence of negatively charged subunits. Figure 5 shows a significant trend to increasing binding scores with an increasing number of glutamate/aspartate subunits. In the verification

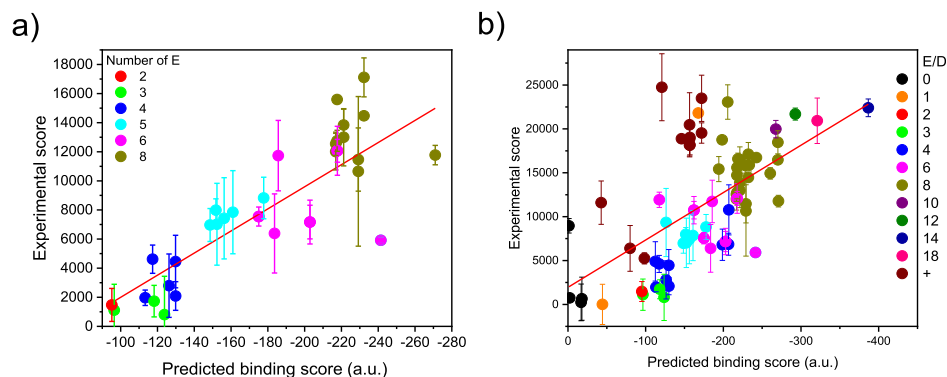


Figure 5. Comparison of the theoretically and the experimentally obtained binding scores for amino acid sequences with different quantities of negatively charged amino acid groups and different arrangements of negatively charged amino acid groups. The numbers in the legend accord with the number of negatively charged amino acid residues in the peptide linked to the surface. Glutamate containing peptides with a maximal length of eight subunits are illustrated on the left (a) whereas the entire membrane is plotted on the right. Not only negatively charged peptides have been investigated. A detailed table is listed in the [Supporting Information](#). The + in the legend refers to peptides which consist solely of positively charged subunits.

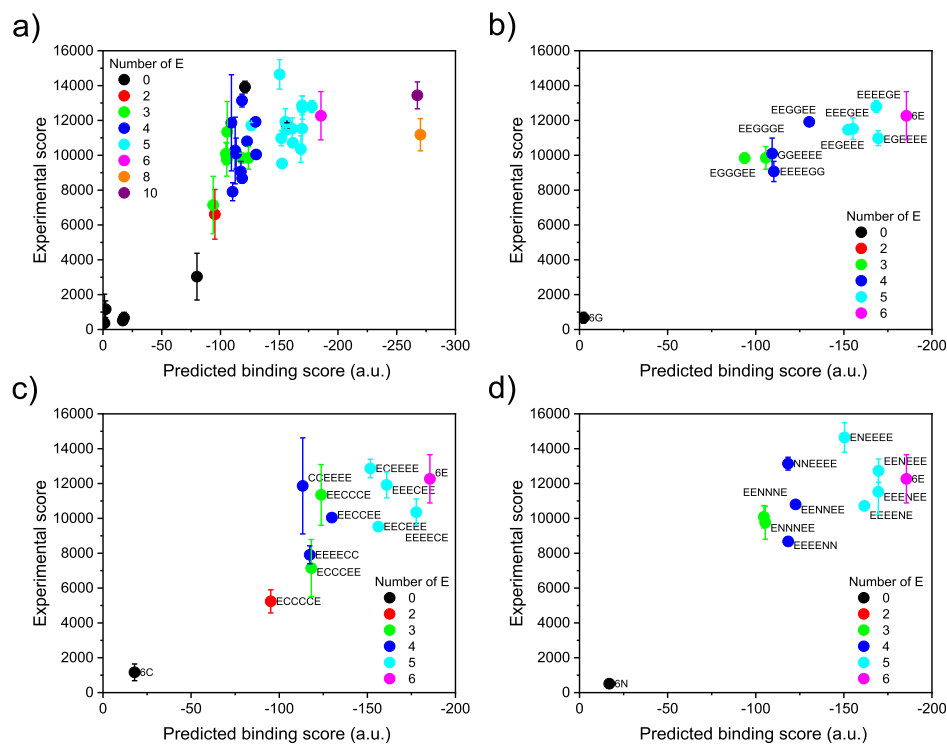


Figure 6. Comparison of the theoretically and the experimentally obtained binding scores for peptide sequences with different amounts and different arrangements of glutamate subunits. The whole experimental data set for the glutamate containing membrane is illustrated (a). The conformational and constitutional exchange of glutamate by glycine (b), cysteine (c), and asparagine (d) is shown here.

experiments, the binding scores of positively charged peptides were higher than predicted and expected based on previous experiments (Figure 5b).¹² In general, we find that the contribution of uncharged amino acids only weakly affects binding to magnetite nanoparticles; the binding scores of such peptides differ little from those of similar charged peptides. However, it is interesting that both positively and negatively charged amino acids bind magnetic nanoparticles to a similar extent, which indicates that the heterogeneous particle surface is well described by the model. This behavior can be observed in the model results as well as in those of the experiment. Overall, the parameterization of the model on the homo peptides appears to be quite transferable to other systems. We

do not, however, propose unexpected synergistic or entropic effects.

From the observations above, we can derive a few rules to design peptides that bind well to magnetite nanoparticle binding tags under the investigated conditions. First, the focus should be on negatively or positively charged binding tags, that is the binding should usually be induced by electrostatic interactions between the surface and the peptide.^{25,52,54} These observations match our previous results for the binding of amino acids and peptides to agglomerated IONs, which we found to be strongly influenced by the zeta potential and the surface potential of nanoparticles and therefore strongly dependent on the environment.^{12,51,52} However, it has to be

score still results for two glycine molecules in the middle of the hexamer, but here terminal glycine on the membrane leads to an even higher binding score. The prediction model can be validated with these experiments even though some unexpected results might lead to new thought provoking impulses for peptide design. Our model and the experiments predict a slightly better binding behavior of more flexible peptides and a slightly worse binding for cysteine containing peptides. It is difficult to extrapolate a theory of specific cysteine binding to the IONs in our system. Furthermore, the strong influence of electrostatics in bio–nano interactions can be verified here in theory and experiment.

CONCLUSIONS

The development of concepts to model, understand, and ultimately predict bio–nano interactions is important to further expand their applications. Presently, this challenge is hindered by the fact that peptide synthesis is expensive and analytical methods are lacking to accurately measure individual amino acid adsorption energies. On the other hand, the conformational flexibility and the complex interactions of even medium sized peptides with surfaces complicate all atom molecular dynamics simulations of such systems. We therefore investigated whether parameters determined experimentally for a certain subset of peptides can be transferred to other peptides. For this purpose, we have developed an EISM. This model, based on various force field components for several interaction contributions, contains effective parameters that can be adjusted to fit the behavior of a set of peptides. From binding experiments of agglomerated magnetite nanoparticles to different peptides anchored to a cellulose membrane, model parameters can be estimated for 20 amino acids. Here, EISM is validated for peptide binding to magnetite nanoparticles in Tris buffer, but the principle can be applied to various buffers and materials. By generating experimental binding data, the model was parameterized, and the surface accessible area (SASA) force field contribution term based on these experiments can be used to predict trends in the binding of a wide variety of peptides within the uncertainty of the experimental measurements. For the investigated ION surfaces, we identified binding peptides which might be used as affinity tags for protein purification.²⁵ Electrostatic contributions of positively and negatively charged amino acid side chains can be foreseen as well as the effects of adding various other amino acids. An example for these effects is the substitution of glutamate with glycine, which adds flexibility to the peptide, leading to higher predicted binding scores. These predicted binding patterns have been verified with additional binding experiments where higher predicted binding scores lead to higher experimental binding scores. Thus, the development of a new functional tool for the prediction of a peptide binding to complex nanoscale surfaces, such as magnetite, has been demonstrated. Accordingly, the EISM should facilitate the development of new affinity peptides for various surfaces, which may be used for sensing, downstream processing or even drug delivery applications.

ASSOCIATED CONTENT

Supporting Information

The Supporting Information is available free of charge on the ACS Publications website at DOI: 10.1021/acs.langmuir.9b00729.

Dynamic light scattering of particle agglomerates, and summary of peptide arrays (PDF)

AUTHOR INFORMATION

Corresponding Authors

*E mail: s.berensmeier@tum.de (S.B.).

*E mail: wolfgang.wenzel@kit.edu (W.W.).

ORCID

Sebastian Patrick Schwaminger: 0000 0002 8627 0807

Silvia Angela Blank-Shim: 0000 0003 0239 8545

Author Contributions

The article was written through contributions of all the authors. All the authors have given approval to the final version of the article.

Notes

The authors declare no competing financial interest.

ACKNOWLEDGMENTS

We are particularly appreciative for the financial support of this work by the Federal Ministry of Education and Research (grant numbers 031A173A and 031A173B).

REFERENCES

- (1) Ling, D.; Hyeon, T. Chemical Design of Biocompatible Iron Oxide Nanoparticles for Medical Applications. *Small* **2013**, *9*, 1450–1466.
- (2) Peelle, B. R.; Krauland, E. M.; Wittrup, K. D.; Belcher, A. M. Design Criteria for Engineering Inorganic Material Specific Peptides. *Langmuir* **2005**, *21*, 6929–6933.
- (3) Penna, M.; Ley, K.; Maclaughlin, S.; Yarovsky, I. Surface Heterogeneity: A Friend or Foe of Protein Adsorption Insights from Theoretical Simulations. *Faraday Discuss.* **2016**, *191*, 435–464.
- (4) Monopoli, M. P.; Åberg, C.; Salvati, A.; Dawson, K. A. Biomolecular Coronas Provide the Biological Identity of Nanosized Materials. *Nat. Nanotechnol.* **2012**, *7*, 779.
- (5) Slocik, J. M.; Naik, R. R. Probing Peptide Nanomaterial Interactions. *Chem. Soc. Rev.* **2010**, *39*, 3454–3463.
- (6) Maity, S.; Zanuy, D.; Razvag, Y.; Das, P.; Alemán, C.; Reches, M. Elucidating the Mechanism of Interaction between Peptides and Inorganic Surfaces. *Phys. Chem. Chem. Phys.* **2015**, *17*, 15305–15315.
- (7) Tinberg, C. E.; Khare, S. D.; Dou, J.; Doyle, L.; Nelson, J. W.; Schena, A.; Jankowski, W.; Kalodimos, C. G.; Johnsson, K.; Stoddard, B. L.; Baker, D. Computational Design of Ligand Binding Proteins with High Affinity and Selectivity. *Nature* **2013**, *501*, 212.
- (8) Schmidt, T. G. M.; Skerra, A. The Strep Tag System for One Step Purification and High Affinity Detection or Capturing of Proteins. *Nat. Protoc.* **2007**, *2*, 1528–1535.
- (9) Colombo, M.; Carregal Romero, S.; Casula, M. F.; Gutiérrez, L.; Morales, M. P.; Böhm, I. B.; Heverhagen, J. T.; Prosperi, D.; Parak, W. J. Biological Applications of Magnetic Nanoparticles. *Chem. Soc. Rev.* **2012**, *41*, 4306–4334.
- (10) Mikhaylov, G.; Mikac, U.; Magaeva, A. A.; Itin, V. I.; Naiden, E. P.; Psakhye, I.; Babes, L.; Reinheckel, T.; Peters, C.; Zeiser, R.; Bogoy, M.; Turk, V.; Psakhye, S. G.; Turk, B.; Vasiljeva, O. Ferri Liposomes as an MRI Visible Drug Delivery System for Targeting Tumours and their Microenvironment. *Nat. Nanotechnol.* **2011**, *6*, 594–602.
- (11) Lichty, J. J.; Malecki, J. L.; Agnew, H. D.; Michelson Horowitz, D. J.; Tan, S. Comparison of Affinity Tags for Protein Purification. *Protein Expression Purif.* **2005**, *41*, 98–105.
- (12) Blank Shim, S. A.; Schwaminger, S. P.; Borkowska Panek, M.; Anand, P.; Yamin, P.; Fraga García, P.; Fink, K.; Wenzel, W.; Berensmeier, S. Binding Patterns of Homo Peptides on Bare Magnetic Nanoparticles: Insights into Environmental Dependence. *Sci. Rep.* **2017**, *7*, 14047.

- (13) Laurent, S.; Forge, D.; Port, M.; Roch, A.; Robic, C.; Vander Elst, L.; Muller, R. N. Magnetic Iron Oxide Nanoparticles: Synthesis, Stabilization, Vectorization, Physicochemical Characterizations, and Biological Applications. *Chem. Rev.* **2008**, *108*, 2064–2110.
- (14) Levy, M.; Quarta, A.; Espinosa, A.; Figuerola, A.; Wilhelm, C.; García Hernández, M.; Genovese, A.; Falqui, A.; Alloyeau, D.; Buonsanti, R.; Cozzoli, P. D.; García, M. A.; Gazeau, F.; Pellegrino, T. Correlating Magneto Structural Properties to Hyperthermia Performance of Highly Monodisperse Iron Oxide Nanoparticles Prepared by a Seeded Growth Route. *Chem. Mater.* **2011**, *23*, 4170–4180.
- (15) Mahmoudi, M.; Serpooshan, V.; Laurent, S. Engineered Nanoparticles for Biomolecular Imaging. *Nanoscale* **2011**, *3*, 3007–3026.
- (16) Lee, N.; Hyeon, T. Designed Synthesis of Uniformly Sized Iron Oxide Nanoparticles for Efficient Magnetic Resonance Imaging Contrast Agents. *Chem. Soc. Rev.* **2012**, *41*, 2575–2589.
- (17) Roth, H. C.; Schwaminger, S. P.; Peng, F.; Berensmeier, S. Immobilization of Cellulase on Magnetic Nanocarriers. *ChemistryOpen* **2016**, *5*, 183–187.
- (18) Schwaminger, S. P.; Fraga García, P.; Selbach, F.; Hein, F. G.; Fuß, E. C.; Surya, R.; Roth, H. C.; Blank Shim, S. A.; Wagner, F. E.; Heissler, S.; Berensmeier, S. Bio Nano Interactions: Cellulase on Iron Oxide Nanoparticle Surfaces. *Adsorption* **2017**, *23*, 281–292.
- (19) Schnell, F.; Kube, M.; Berensmeier, S.; Schwaminger, S. P. Magnetic Recovery of Cellulase from Cellulose Substrates with Bare Iron Oxide Nanoparticles. *ChemNanoMat* **2019**, *5*, 422.
- (20) Malmsten, M. Inorganic Nanomaterials as Delivery Systems for Proteins, Peptides, DNA, and siRNA. *Curr. Opin. Colloid Interface Sci.* **2013**, *18*, 468–480.
- (21) Fraga García, P.; Brammen, M.; Wolf, M.; Reinlein, S.; Freiherr von Roman, M.; Berensmeier, S. High Gradient Magnetic Separation for Technical Scale Protein Recovery Using Low Cost Magnetic Nanoparticles. *Sep. Purif. Technol.* **2015**, *150*, 29–36.
- (22) Hong, J. W.; Studer, V.; Hang, G.; Anderson, W. F.; Quake, S. R. A Nanoliter Scale Nucleic Acid Processor with Parallel Architecture. *Nat. Biotechnol.* **2004**, *22*, 435–439.
- (23) Schwaminger, S. P.; Fraga García, P.; Blank Shim, S. A.; Straub, T.; Haslbeck, M.; Muraca, F.; Dawson, K. A.; Berensmeier, S. Magnetic One Step Purification of His Tagged Protein by Bare Iron Oxide Nanoparticles. *ACS Omega* **2019**, *4*, 3790–3799.
- (24) Pan, Y.; Du, X.; Zhao, F.; Xu, B. Magnetic Nanoparticles for the Manipulation of Proteins and Cells. *Chem. Soc. Rev.* **2012**, *41*, 2912–2942.
- (25) Schwaminger, S. P.; Blank Shim, S. A.; Scheifele, I.; Pipich, V.; Fraga García, P.; Berensmeier, S. Design of Interactions Between Nanomaterials and Proteins: A Highly Affine Peptide Tag to Bare Iron Oxide Nanoparticles for Magnetic Protein Separation. *Biotechnol J.* **2019**, *14*, No. e1800055.
- (26) Schwaminger, S.; Blank Shim, S. A.; Borkowska Panek, M.; Anand, P.; Fraga García, P.; Fink, K.; Wenzel, W.; Berensmeier, S. Experimental Characterization and Simulation of Amino Acid and Peptide Interactions with Inorganic Materials. *Eng. Life Sci.* **2018**, *18*, 84.
- (27) Mahmoudi, M.; Lynch, I.; Ejtehadi, M. R.; Monopoli, M. P.; Bombelli, F. B.; Laurent, S. Protein–Nanoparticle Interactions: Opportunities and Challenges. *Chem. Rev.* **2011**, *111*, 5610–5637.
- (28) Nel, A. E.; Mädler, L.; Velegol, D.; Xia, T.; Hoek, E. M. V.; Somasundaran, P.; Klaessig, F.; Castranova, V.; Thompson, M. Understanding Biophysicochemical Interactions at the Nano Bio Interface. *Nat. Mater.* **2009**, *8*, 543–557.
- (29) Tamerler, C.; Sarikaya, M. Genetically Designed Peptide Based Molecular Materials. *ACS Nano* **2009**, *3*, 1606–1615.
- (30) Wang, L.; Wu, Y.; Deng, Y.; Kim, B.; Pierce, L.; Krilov, G.; Lypyan, D.; Robinson, S.; Dahlgren, M. K.; Greenwood, J.; Romero, D. L.; Masse, C.; Knight, J. L.; Steinbrecher, T.; Beuming, T.; Damm, W.; Harder, E.; Sherman, W.; Brewer, M.; Wester, R.; Murcko, M.; Frye, L.; Farid, R.; Lin, T.; Mobley, D. L.; Jorgensen, W. L.; Berne, B. J.; Friesner, R. A.; Abel, R. Accurate and Reliable Prediction of Relative Ligand Binding Potency in Prospective Drug Discovery by Way of a Modern Free Energy Calculation Protocol and Force Field. *J. Am. Chem. Soc.* **2015**, *137*, 2695–2703.
- (31) Henzler Wildman, K.; Kern, D. Dynamic Personalities of Proteins. *Nature* **2007**, *450*, 964.
- (32) Anand, P.; Borkowska Panek, M.; Gussmann, F.; Fink, K.; Wenzel, W. Modelling Peptide Adsorption on Inorganic Surfaces. *Lect. Notes Comput. Sci.* **2016**, *9859*, 339–340.
- (33) Strunk, T.; Wolf, M.; Brieg, M.; Klenin, K.; Biewer, A.; Tristram, F.; Ernst, M.; Kleine, P. J.; Heilmann, N.; Kondov, I.; Wenzel, W. SIMONA 1.0: An Efficient and Versatile Framework for Stochastic Simulations of Molecular and Nanoscale Systems. *J. Comput. Chem.* **2012**, *33*, 2602–2613.
- (34) Tribello, G. A.; Bonomi, M.; Branduardi, D.; Camilloni, C.; Bossi, G. PLUMED 2: New Feathers for an Old Bird. *Comput. Phys. Commun.* **2014**, *185*, 604–613.
- (35) Costa, D.; Garrain, P. A.; Baaden, M. Understanding Small Biomolecule Biomaterial Interactions: A Review of Fundamental Theoretical and Experimental Approaches for Biomolecule Interactions with Inorganic Surfaces. *J. Biomed. Mater. Res., Part A* **2013**, *101*, 1210–1222.
- (36) Vallee, A.; Humblot, V.; Pradier, C. M. Peptide Interactions with Metal and Oxide Surfaces. *Acc. Chem. Res.* **2010**, *43*, 1297–1306.
- (37) Rimola, A.; Aschi, M.; Orlando, R.; Ugliengo, P. Does Adsorption at Hydroxyapatite Surfaces Induce Peptide Folding? Insights from Large Scale B3LYP Calculations. *J. Am. Chem. Soc.* **2012**, *134*, 10899–10910.
- (38) Emami, F. S.; Puddu, V.; Berry, R. J.; Varshney, V.; Patwardhan, S. V.; Perry, C. C.; Heinz, H. Force Field and a Surface Model Database for Silica to Simulate Interfacial Properties in Atomic Resolution. *Chem. Mater.* **2014**, *26*, 2647–2658.
- (39) Emami, F. S.; Puddu, V.; Berry, R. J.; Varshney, V.; Patwardhan, S. V.; Perry, C. C.; Heinz, H. Prediction of Specific Biomolecule Adsorption on Silica Surfaces as a Function of pH and Particle Size. *Chem. Mater.* **2014**, *26*, 5725–5734.
- (40) Okochi, M.; Sugita, T.; Furusawa, S.; Umetsu, M.; Adschiri, T.; Honda, H. Peptide Array Based Characterization and Design of ZnO High Affinity Peptides. *Biotechnol. Bioeng.* **2010**, *106*, 845–851.
- (41) Kuboyama, M.; Kato, R.; Okochi, M.; Honda, H. Screening for Silver Nanoparticle Binding Peptides by Using a Peptide Array. *Biochem. Eng. J.* **2012**, *66*, 73–77.
- (42) Okochi, M.; Ogawa, M.; Kaga, C.; Sugita, T.; Tomita, Y.; Kato, R.; Honda, H. Screening of Peptides with a High Affinity for ZnO Using Spot Synthesized Peptide Arrays and Computational Analysis. *Acta Biomater.* **2010**, *6*, 2301–2306.
- (43) Roth, H. C.; Schwaminger, S. P.; Schindler, M.; Wagner, F. E.; Berensmeier, S. Influencing factors in the CO precipitation process of superparamagnetic iron oxide nano particles: A model based study. *J. Magn. Magn. Mater.* **2015**, *377*, 81–89.
- (44) Brand, N. Protein Protein Interactions: A Molecular Cloning Manual. By Erica A. Golemis and Peter D. Adams (Eds.). *Proteomics* **2006**, *6*, 6119–6120.
- (45) Setzler, J.; Seith, C.; Brieg, M.; Wenzel, W. SLIM: An Improved Generalized Born Implicit Membrane Model. *J. Comput. Chem.* **2014**, *35*, 2027–2039.
- (46) Lindorff Larsen, K.; Piana, S.; Palmo, K.; Maragakis, P.; Klepeis, J. L.; Dror, R. O.; Shaw, D. E. Improved side chain torsion potentials for the Amber ff99SB protein force field. *Proteins: Struct., Funct., Bioinf.* **2010**, *78*, 1950–1958.
- (47) Piana, S.; Klepeis, J. L.; Shaw, D. E. Assessing the Accuracy of Physical Models Used in Protein Folding Simulations: Quantitative Evidence from Long Molecular Dynamics Simulations. *Curr. Opin. Struct. Biol.* **2014**, *24*, 98–105.
- (48) Brieg, M.; Setzler, J.; Albert, S.; Wenzel, W. Generalized Born Implicit Solvent Models for Small Molecule Hydration Free Energies. *Phys. Chem. Chem. Phys.* **2017**, *19*, 1677–1685.
- (49) Klenin, K. V.; Tristram, F.; Strunk, T.; Wenzel, W. Derivatives of Molecular Surface Area and Volume: Simple and Exact Analytical Formulas. *J. Comput. Chem.* **2011**, *32*, 2647–2653.

- (50) Schwaminger, S. P.; Bauer, D.; Fraga García, P.; Wagner, F. E.; Berensmeier, S. Oxidation of Magnetite Nanoparticles: Impact on Surface and Crystal Properties. *CrystEngComm* **2017**, *19*, 246–255.
- (51) Schwaminger, S. P.; Fraga García, P.; Merck, G. K.; Bodensteiner, F. A.; Heissler, S.; Günther, S.; Berensmeier, S. Nature of Interactions of Amino Acids with Bare Magnetite Nanoparticles. *J. Phys. Chem. C* **2015**, *119*, 23032–23041.
- (52) Schwaminger, S. P.; Blank Shim, S. A.; Scheifele, I.; Fraga García, P.; Berensmeier, S. Peptide Binding to Metal Oxide Nanoparticles. *Faraday Discuss.* **2017**, *204*, 233–250.
- (53) Kupcik, R.; Rehulka, P.; Bilkova, Z.; Sopha, H.; Macak, J. M. New Interface for Purification of Proteins: One Dimensional TiO₂ Nanotubes Decorated by Fe₃O₄ Nanoparticles. *ACS Appl. Mater. Interfaces* **2017**, *9*, 28233–28242.
- (54) Sano, K. I.; Shiba, K. A Hexapeptide Motif that Electrostatically Binds to the Surface of Titanium. *J. Am. Chem. Soc.* **2003**, *125*, 14234–14235.
- (55) Reddy Chichili, V. P.; Kumar, V.; Sivaraman, J. Linkers in the Structural Biology of Protein Protein Interactions. *Protein Sci.* **2013**, *22*, 153–167.
- (56) Cohen, H.; Gedanken, A.; Zhong, Z. One Step Synthesis and Characterization of Ultrastable and Amorphous Fe₃O₄ Colloids Capped with Cysteine Molecules. *J. Phys. Chem. C* **2008**, *112*, 15429–15438.
- (57) Kiedziarska, A.; Czepczynska, H.; Smietana, K.; Otlewski, J. Expression, Purification and Crystallization of Cysteine Rich Human Protein Muskeln in Escherichia coli. *Protein Expression Purif.* **2008**, *60*, 82–88.
- (58) Vieira, A. P.; Berndt, G.; de Souza Junior, I. G.; Di Mauro, E.; Paesano, A.; de Santana, H.; da Costa, A. C. S.; Zaia, C. T. B. V.; Zaia, D. A. M. Adsorption of cysteine on hematite, magnetite and ferrihydrite: FT IR, Mössbauer, EPR spectroscopy and X ray diffractometry studies. *Amino Acids* **2011**, *40*, 205–214.